Appendix A.50:

Palinurus Rd 1 – VsVp 57185

Table 1: Site Description for Palinurus Rd 1 (VsVp 57185).

Attribute	Yes/No		Description/Date	Symbol in Figure 1
	10-m Buffer	20-m Buffer		
Near a body of surface water or other free face features?	No	No	The center of the site is ~70 m to the SW from the unnamed stream (the free-face height is ~1 m) and ~290 m to the NE from the Heathcote River (the free-face height is ~2.5 m).	NA
Lateral spreading observed during the CES?	No	No	No lateral spreading was observed by the mapping team.[1]	NA
Nearby buildings or structures?	No	Yes	Building coverage of the 20-m buffer is 1%. The building is in the SW quadrant of the 20-m buffer.	White Fill + Brown Outline
Sloping land?	No	No	Level ground, open field	NA
Step changes in the ground surface?	No	No	Uneven surface (paddock), soil mounds	NA
Retaining walls?	No	No	NA	NA
Vegetation?	No	Yes	Trees and bushes cover 3% of the 20-m buffer. They are in the SW quadrant of the 20-m buffer.	White Fill + Green Outline
Anthropogenic changes to the site between the LiDAR surveys?	Yes	Yes	Land resurfacing in both buffers between Aug 2014 and Jan 2016.	NA
Other important factors?	Yes	Yes	The paddock is subject to land resurfacing.	NA

Note: Buffer is the area within a circle of a specified radius with VsVp investigations done at its center (172.688215°, -43.551331°).

[1] Canterbury Geotechnical Database. (2012). "Observed Ground Crack Locations", Map Layer CGD0400 - 23 July 2012, retrieved July 09, 2018 from https://canterburygeotechnicaldatabase.projectorbit.com/

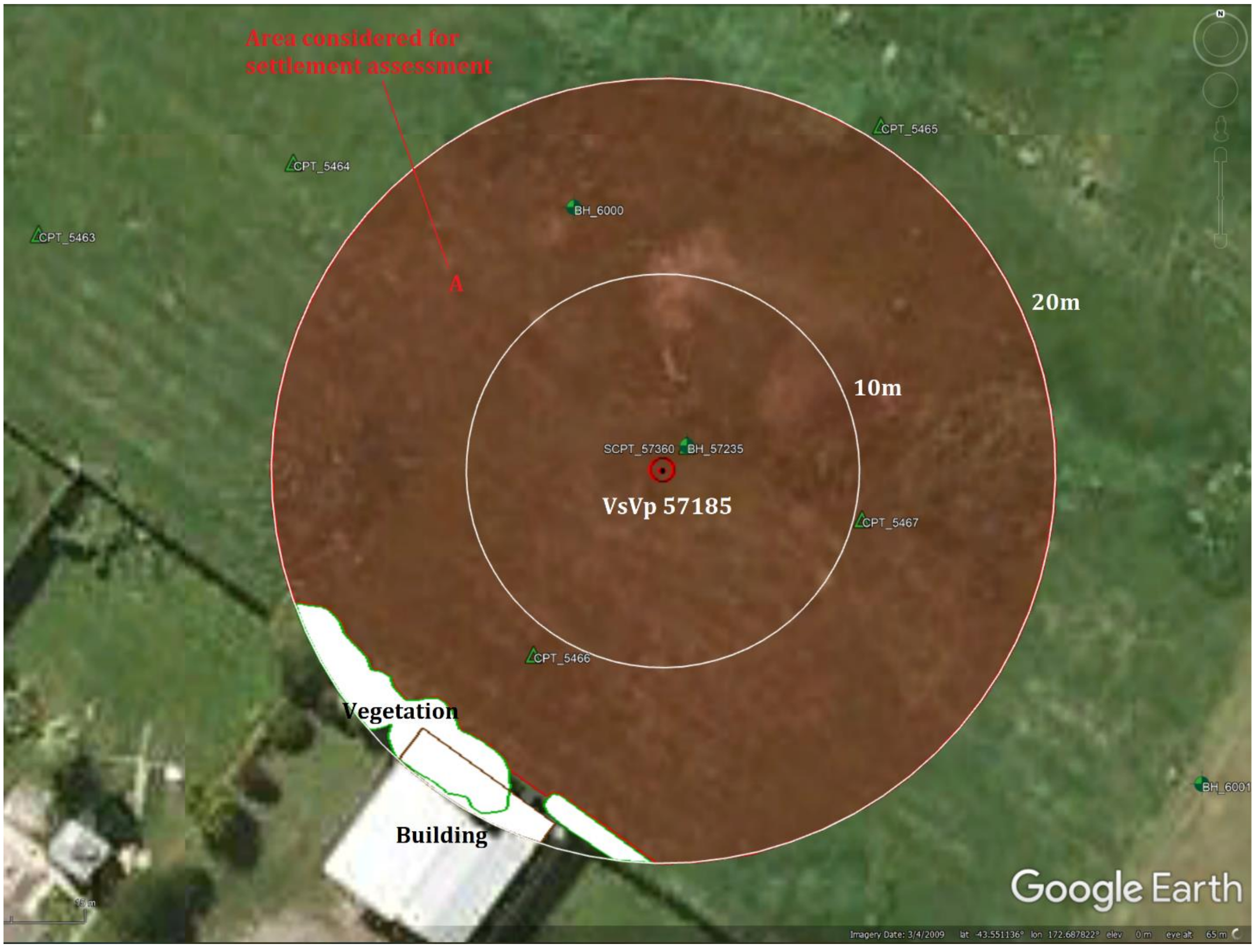

Figure 1: Site plan with areas where ejecta-induced settlement is considered.

Note 1: Patch A in the free field was selected for settlement assessment as an area free of vegetation and structures. Other important factors considered in the patch selection were its proximity to a CPT, a property subjected to addition and/or demolition of a structure, front yard/backyard alterations (e.g., ploughing, rubble, scrap), and aerial distribution of sediment ejecta. The LiDAR-based ejecta-induced settlement was not estimated for any earthquake event due to the evident absence of ejecta.

Table 2: LiDAR flight error adjustments, global adjustments for the difference between average LiDAR point elevations and benchmark survey elevations, and vertical tectonic movement adjustments.

	Adjustments (mm)		
Earthquake Event(s)	LiDAR Flight Error	Global Offset[2]	Tectonic Vertical Movement
Sep-10	NA	-3	0
Feb-11	NA	16	+320
Jun-11	0	38	-30
Dec-11	-50	-65	+25
CES	-50	-14	+315
Any LiDAR survey affected by ejecta?			No

Note: The negative sign indicates the subtraction from the ground surface subsidence, while the positive sign indicates the addition to the ground surface subsidence.

Table 3: LiDAR Measurement Error for Patch A.

Surveys	Buffer	Area Averaged Difference Indicating Repeat Measurement Error (mm)	$\sigma^*_{\text{individual LiDAR points}}$ (mm)	%Reduction in σ due to Area Averaging of LiDAR Points
Post Feb 2011: Mar 2011 and May 2011	10-m	ND	59	[ND,ND]
	20-m	ND		
Post Dec 2011: Feb 2012 and Oct 2015	10-m	ND	70	[ND,ND]
	20-m	ND		

*Standard deviation; ND = Not determined.

Table 4: Ground surface subsidence adjustments due to LiDAR measurement error for Patch A.

Earthquake Event(s)	$\sigma_{\text{pre-EQ LiDAR survey}}$ (mm)	$\sigma_{\text{post-EQ LiDAR survey}}$ (mm)	σ_{total} (mm)	Area Average Adjusted σ (mm) **
Sep-10	158	56	134	ND
Feb-11	56	59	59	ND
Jun-11	59	61	62	ND
Dec-11	61	70	87	ND
CES	158	70	124	ND

**Based on the highest %Reduction in Table 3; ND = Not determined due to topographic features.

[2] Russell, J., & van Ballegooy, S. (2015). *Canterbury Earthquake Sequence: Increased liquefaction vulnerability assessment methodology*. New Zealand: Tonkin & Taylor Ltd.

Table 5: Raw liquefaction-related ground surface subsidence using original LiDAR points for Patch A.

Earthquake Event(s)	Average Ground Surface Subsidence (mm) 10-m Buffer	20-m Buffer
Sep-10	NA	NA
Feb-11	NA	NA
Jun-11	ND	ND
Dec-11	ND	ND
CES	ND	ND

NA = Not available; ND = Not determined.

Table 6: Corrected liquefaction-related ground surface subsidence using original LiDAR points for Patch A with the calculated adjustments in Table 2.

Earthquake Event(s)	Average Calculated Ground Surface Subsidence (mm) 10-m Buffer	20-m Buffer
Sep-10	NA	NA
Feb-11	NA	NA
Jun-11	ND	ND
Dec-11	ND	ND
CES	ND	ND

Notes: Plus/minus values are same as those in Table 4a, but rounded to the nearest 25 mm; Positive overall values indicate ground surface subsidence, while negative overall values indicate ground surface uplift; NA = Not available; ND = Not determined.

Table 7: Corrected liquefaction-related ground surface subsidence for Patch A using LiDAR DEMs.

	Estimated Ground Surface Subsidence (mm)					
	10-m Buffer			20-m Buffer		
Earthquake Event(s)	16th %ile	50th %ile	84th %ile	16th %ile	50th %ile	84th %ile
Sep-10	NA	NA	NA	NA	NA	NA
Feb-11	NA	NA	NA	NA	NA	NA
Jun-11	<50	<50	50	<50	<50	50
Dec-11	<50	<50	<50	<50	<50	<50
CES	<50	<50	50	<50	50	100

Note: These percentiles are not the exact statistical measures; they indicate the spatial variability of ground surface subsidence; NA = Not available.

Table 8a: Ejecta-Induced settlement for the top 20 m of the soil profile for Patch A (10-m buffer) for the 50th %ile PGA, P_L=50%, and C_{FC}=0.13 using BI-2014, ZRB-2002, and I_C cutoff of 2.6.

Earthquake Event(s)	M_W	PGA (g)	Depth to Groundwater (m)	S_T (mm)	S_{V1D} (mm)	$S_{E,L}$ (mm)
Sep-10	7.1	0.24	1.3	NA	91±20	NA
Feb-11	6.2	0.68	1.3	NA	253±50	NA
Jun-11	6.2	0.42	1.4	ND	171±25	ND
Dec-11	6.1	0.28	1.5	ND	71±50	ND

Notes: S_T = Total settlement (Table 6); S_{V1D} = Average vertical settlement due to volumetric compression using Boulanger and Idriss (2014) (BI-2014), Zhang et al. (2002) (ZRB-2002) procedures and de Greef and Lengkeek (2018) thin-layer correction; $S_{E,L}$ = Ejecta-induced settlement as the difference between the LiDAR-based S_T and S_{V1D}; NA = Not available; ND = Not determined.

Table 8b: Ejecta-Induced settlement for the top 20 m of the soil profile for Patch A (20-m buffer) for the 50th %ile PGA, P_L=50%, and C_{FC}=0.13 using BI-2014, ZRB-2002, and I_C cutoff of 2.6.

Earthquake Event(s)	M_W	PGA (g)	Depth to Groundwater (m)	S_T (mm)	S_{V1D} (mm)	$S_{E,L}$ (mm)
Sep-10	7.1	0.24	1.3	NA	91±20	NA
Feb-11	6.2	0.68	1.3	NA	250±50	NA
Jun-11	6.2	0.42	1.4	ND	170±25	ND
Dec-11	6.1	0.28	1.5	ND	71±50	ND

Notes: S_T = Total settlement (Table 6); S_{V1D} = Average vertical settlement due to volumetric compression using Boulanger and Idriss (2014) (BI-2014), Zhang et al. (2002) (ZRB-2002) procedures and de Greef and Lengkeek (2018) thin-layer correction; $S_{E,L}$ = Ejecta-induced settlement as the difference between the LiDAR-based S_T and S_{V1D}; NA = Not available; ND = Not determined.

Note 2: The uncertainty for volumetric settlement was derived based on the sensitivity of volumetric settlement to PGA, C_{FC}, and P_L for each earthquake event for VsVp 57203 *Shirley Intermediate School* and CC LIQ 1 – CPT 5586 – *Vivian St* sites. Taking the 50th percentile as the baseline case, the minimum and maximum values corresponding to the difference between the 25th percentile and the 50th percentile and the 75th percentile and the 50th percentile were determined. The arithmetic mean of the range of the minimum and maximum difference was evaluated for each patch at the two sites. The maximum arithmetic mean for each earthquake event was rounded to the nearest five and used as the uncertainty value. Accordingly, the 1-D volumetric settlement uncertainties of ±20, ±50, ±25, and ±50 mm for the Sep-10, Feb-11, Jun-11, and Dec-11 earthquake events, respectively, were used for all sites in this study.

Table 9: Coverage area and height of ejecta estimates for Patch A (10-m and 20-m buffers) using photographs.

Earthquake Event	$A_{E,thick}$ (m^2)	$H_{E,thick}$ (mm)	$A_{E,thin}$ (m^2)	$H_{E,thin}$ (mm)	A_T (m^2)
Sep-10	0	0	0	0	314/1196
Feb-11	0	0	0	0	314/1196
Jun-11	0	0	0	0	314/1196
Dec-11	0	0	0	0	314/1196

Notes: $A_{E,thick/thin}$ = Coverage area of thick/thin ejecta layers; $H_{E,thick/thin}$ = Lower-upper estimate of height of thick/thin ejecta layers; A_T = Total assessment area of a buffer being considered; Thin and thick layers correspond to light gray and dark gray colors of ejecta observed in aerial photographs.

Note 3: The values in Table 9 are based on satellite images and aerial photographs (Figures 8, 9, and 18-21). The ejecta-induced settlement using photographs and engineering judgment, $S_{E,P}$, is estimated as

$$S_{E,P} = \frac{\sum_{i=1}^{a} A_{E,thick,i} * H_{E,thick,i} + \sum_{j=1}^{b} A_{E,thin,j} * H_{E,thin,j}}{A_T} = \frac{\sum_{i=1}^{a} V_{E,thick,i} + \sum_{j=1}^{b} V_{E,thin,j}}{A_T}$$

where

- $A_{E,thick,i}$ and $H_{E,thick,i}$ are the area and the height of a thick ejecta layer, respectively;
- $A_{E,thin,j}$ and $H_{E,thin,j}$ are the area and the height of a thin ejecta layer, respectively;
- A_T is the total assessment area for a buffer being considered (Figure 1).

Table 10: Ejecta-induced settlement estimates for Patch A based on photographs.

Earthquake Event	Patch A (10-m buffer)		Patch A (20-m buffer)	
	$S_{E,P,lower}$ (mm)	$S_{E,P,upper}$ (mm)	$S_{E,P,lower}$ (mm)	$S_{E,P,upper}$ (mm)
Sep-10	0	0	0	0
Feb-11	0	0	0	0
Jun-11	0	0	0	0
Dec-11	0	0	0	0

Note: $S_{E,P,lower}$ and $S_{E,P,upper}$ correspond to lower and upper estimates of $S_{E,P}$, respectively.

Table 11: Best final estimates of ejecta-induced settlement for Patch A.

EQ Event	Patch A (10-m buffer)			Patch A (20-m buffer)		
	$S_{E,L}$ (mm)	$S_{E,P}$ (mm)	$S_{E,final}$ (mm)	$S_{E,L}$ (mm)	$S_{E,P}$ (mm)	$S_{E,final}$ (mm)
Sep-10	NA	0	0	NA	0	0
Feb-11	NA	0	0	NA	0	0
Jun-11	ND	0	0	ND	0	0
Dec-11	ND	0	0	ND	0	0

Notes: $S_{E,L}$ = Ejecta-induced settlement based on LiDAR data reported in Table 8; $S_{E,P}$ = Median ejecta-induced settlement for the range of values reported in Table 10; $S_{E,final}$ = Best final estimate of ejecta-induced settlement rounded to the nearest 5 mm; Final plus/minus values are also rounded to the nearest 5 mm.

Note 4:

- $S_{E,final}$ for Patch A is based solely on $S_{E,P}$ for all earthquake events due to the evident absence of ejecta.
- The Palinurus Rd site is in the zone of slight to moderate LPI overprediction of liquefaction severity for the Sep-10 EQ and severe to excessive LPI overprediction of liquefaction severity for the Feb-11 EQ (Maurer et al. 2014[3]). The LDAT inspection report is not available for the property where the site is located. There are no ground photographs of the site either.

<u>**Summary**</u>:

The best estimate of the ejecta-induced free-field ground settlement at the Palinurus Rd 1 site for the SEP 2010, FEB 2011, JUN 2011, and DEC 2011 earthquake is 0 mm, 0 mm, 0 mm, and 0 mm, respectively.

[3] Maurer, B. W., Green, R. A., Cubrinovski, M., & Bradley, B. A. (2014). Evaluation of the Liquefaction Potential Index for Assessing Liquefaction Hazard in Christchurch, New Zealand. *Journal of Geotechnical and Geoenvironmental Engineering*, 140(7), 04014032-1-11. doi:10.1061/(asce)gt.1943-5606.0001117

Figure 2: Location of the site.

Figure 3: Position of the site relative to nearby buildings, vegetation, and free-face features.

Figure 4: Street view of the level site with uneven ground surface; note the presence of ground mounds and other topographic features.

Figure 5: Satellite image of the site taken in Dec 2004.

Figure 6: Satellite image of the site taken in Jan 2006.

Figure 7: Satellite image of the site taken in Mar 2009.

Figure 8: Satellite image of the site taken on Sep 3, 2010.

Figure 9: Satellite image of the site taken on Sep 5, 2010.

Figure 10: Satellite image of the site taken on Feb 15, 2011.

Figure 11: Satellite image of the site taken on Feb 26, 2011.

Figure 12: Satellite image of the site taken on Mar 8, 2011.

Figure 13: Satellite image of the site taken in Apr 2012.

Figure 14: Satellite image of the site taken in Aug 2014.

Figure 15: Satellite image of the site taken in Jan 2015.

Figure 16: Satellite image of the site taken in Nov 2015.

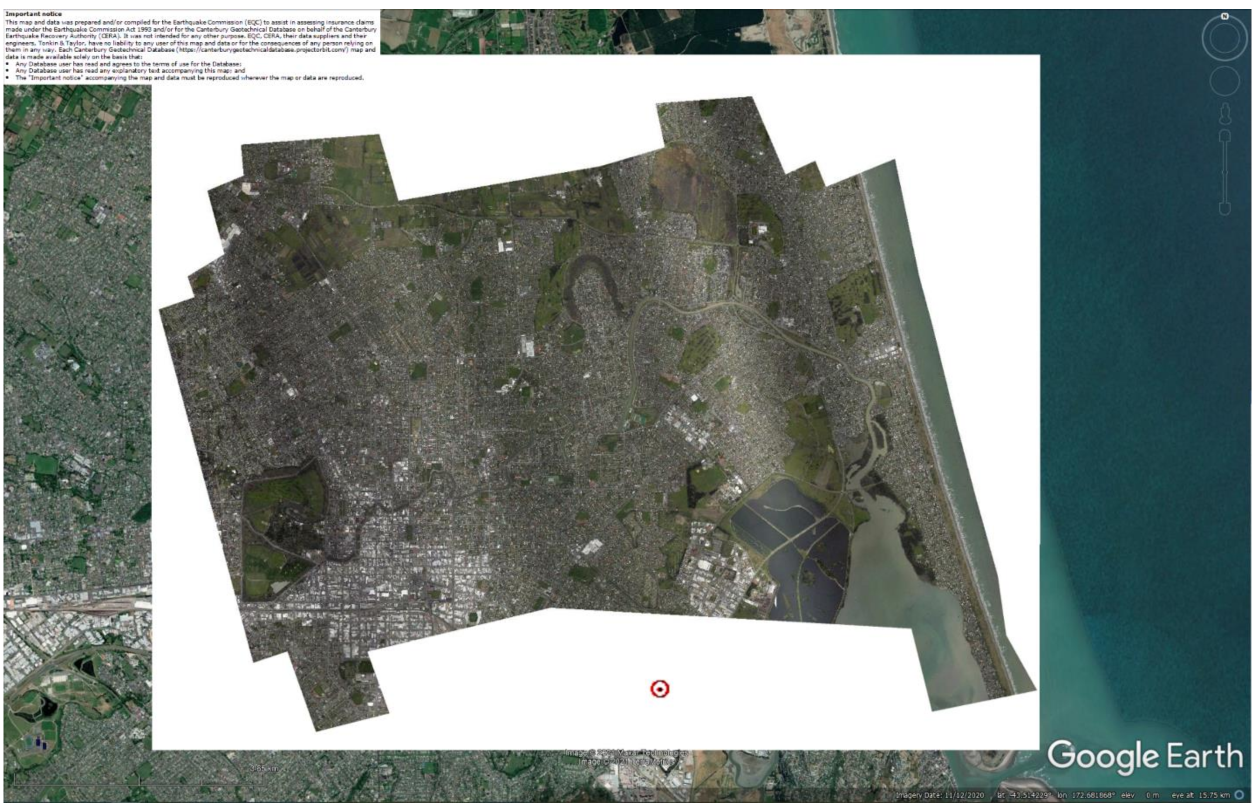

Figure 17: Aerial photograph from Sep 4, 2010, is not available for the site.

Figure 18: Aerial photograph of the site taken on Feb 24, 2011.

Figure 19: Aerial photograph of the site taken on June 14-15, 2011.

Figure 20: Aerial photograph of the site taken on June 16, 2011.

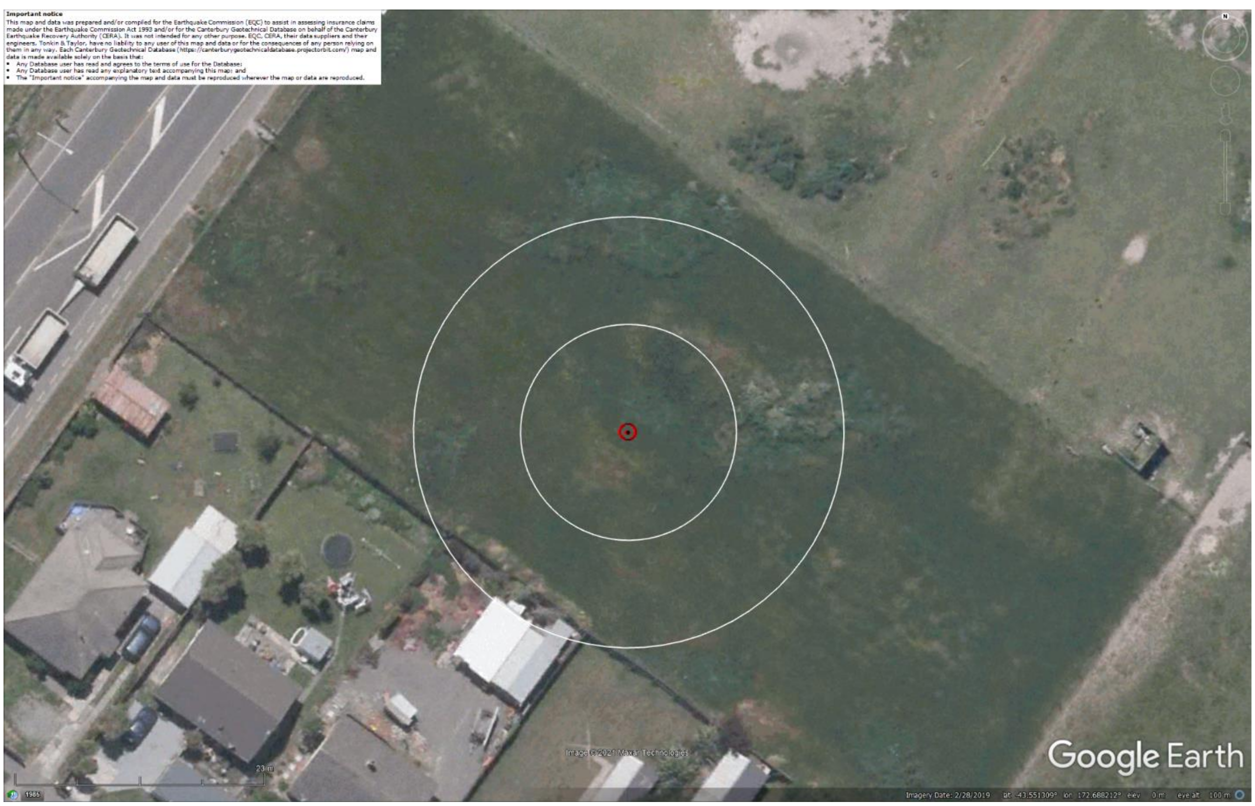

Figure 21: Aerial photograph of the site taken on Dec 24, 2011.

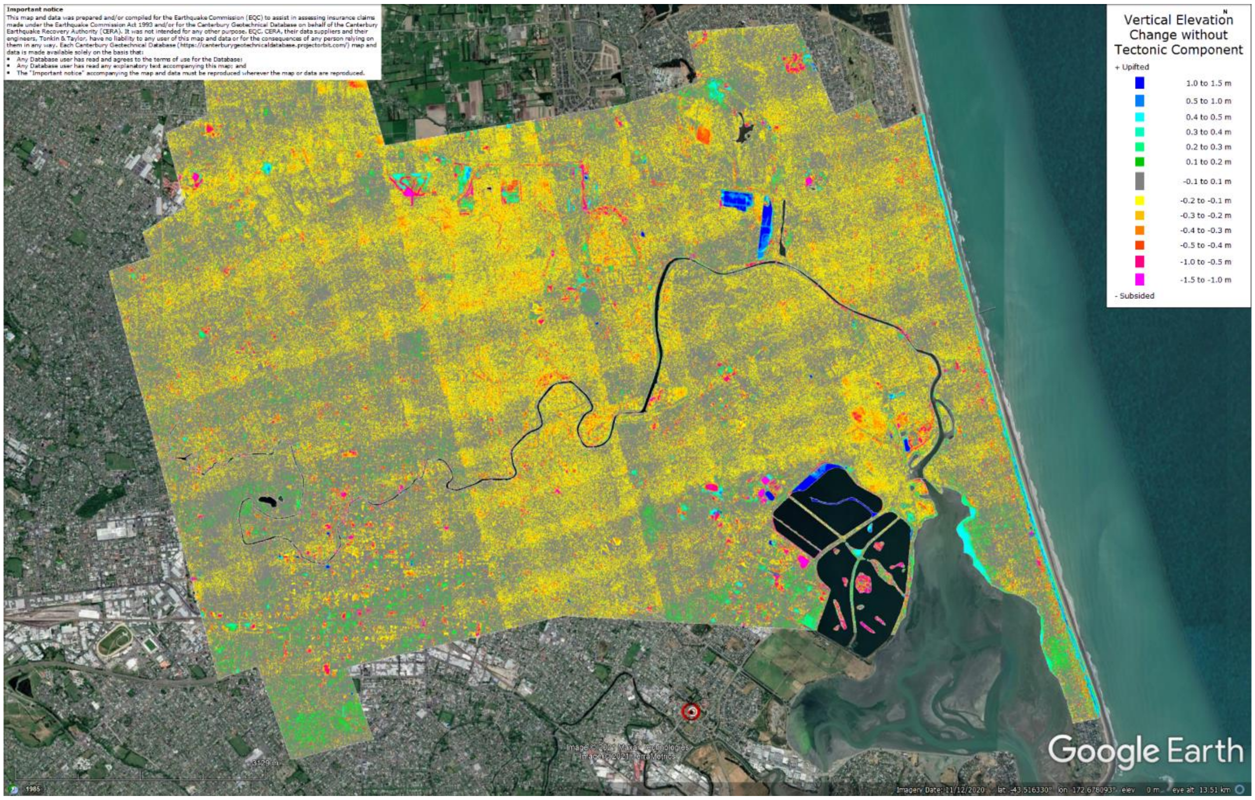

Figure 22: Vertical Ground Movements (Surface – Tectonic) for Sep 2010 Earthquake are not available for the site.

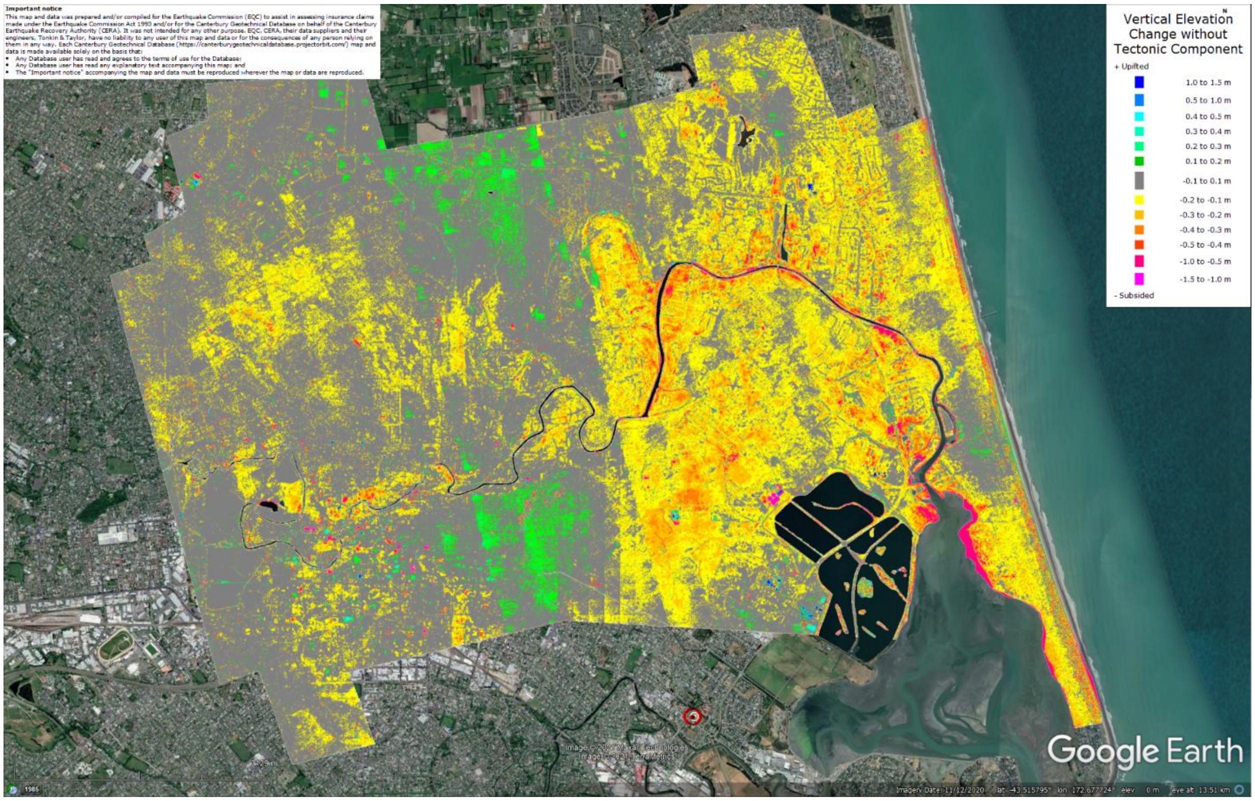

Figure 23: Vertical Ground Movements (Surface – Tectonic) for Feb 2011 Earthquake are not available for the site.

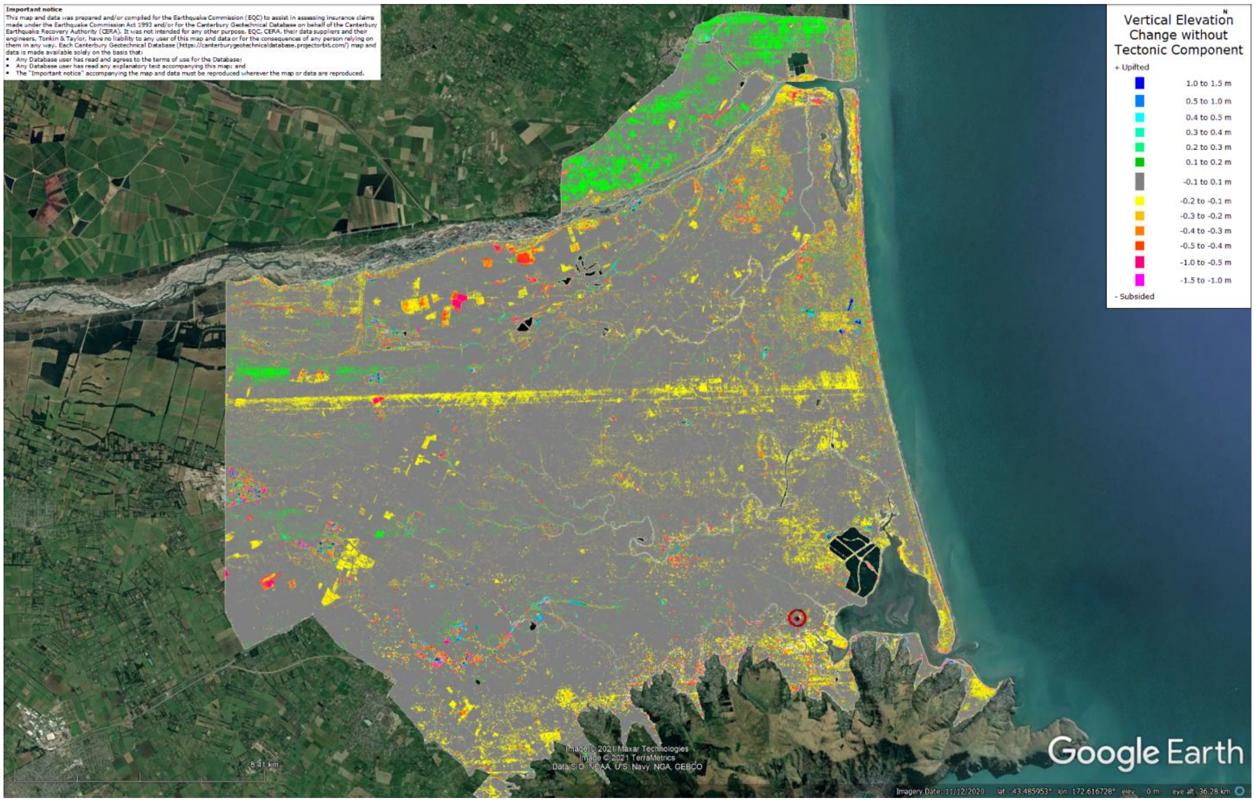

Figure 24: Vertical Ground Movements (Surface – Tectonic) for June 2011 Earthquake – the site is not in the apparent zone of overestimated ground surface subsidence.

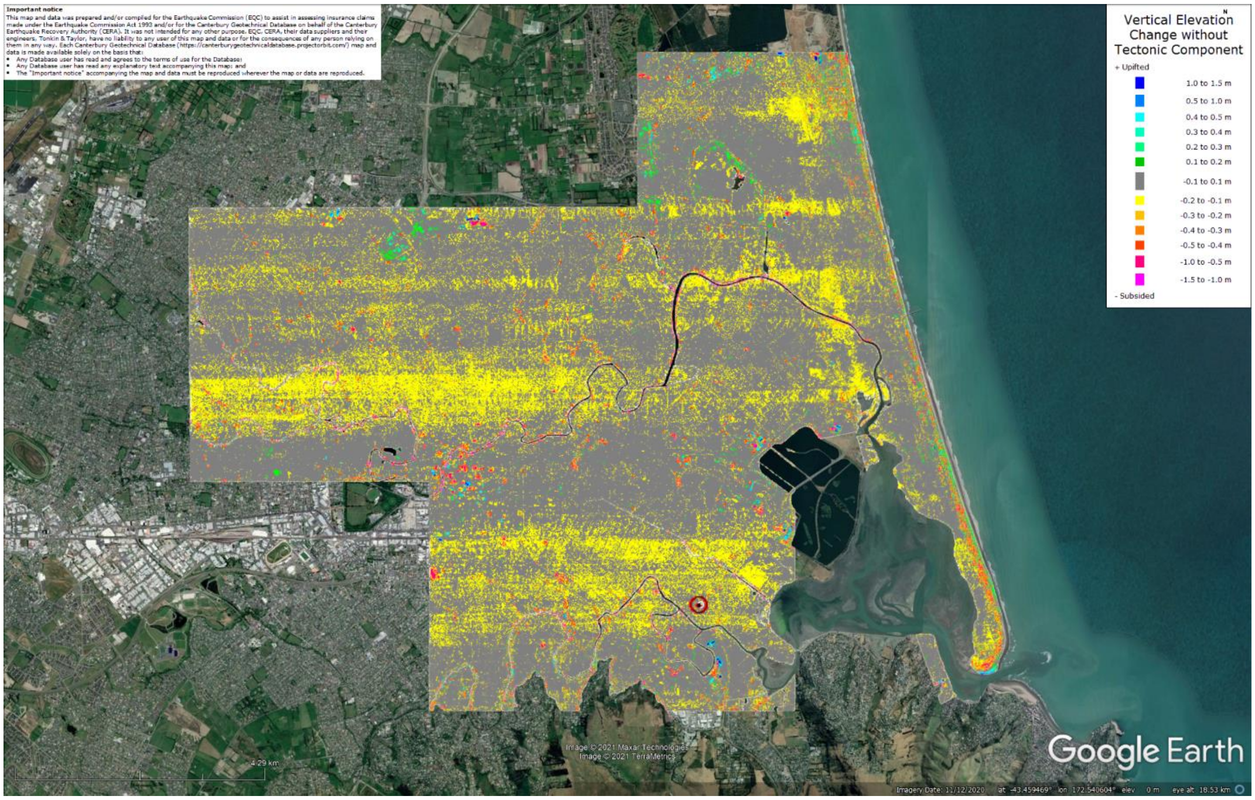

Figure 25: Vertical Ground Movements (Surface – Tectonic) for Dec 2011 Earthquake – the site is in the apparent zone of overestimated ground surface subsidence (i.e., Feb 2012 LiDAR flight error).

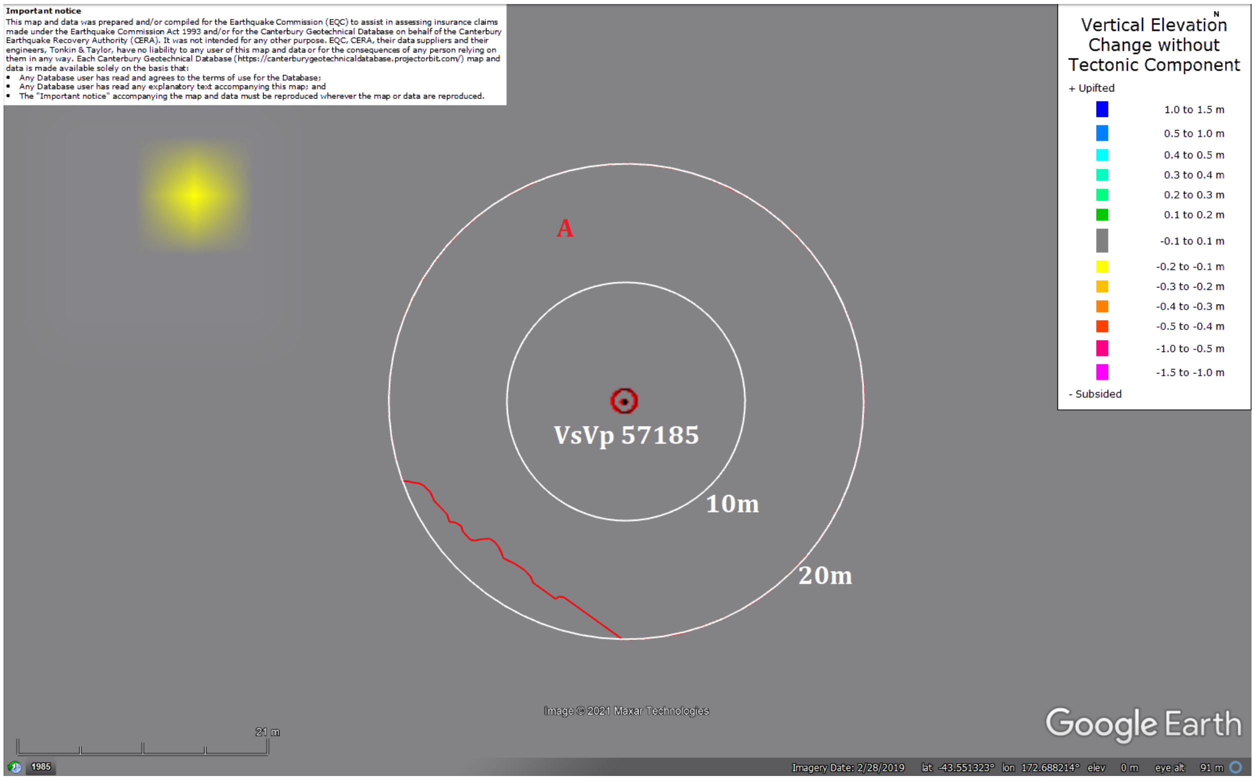

Figure 26: Ground surface subsidence without tectonic component for June 2011 Earthquake according to the LiDAR DEM.

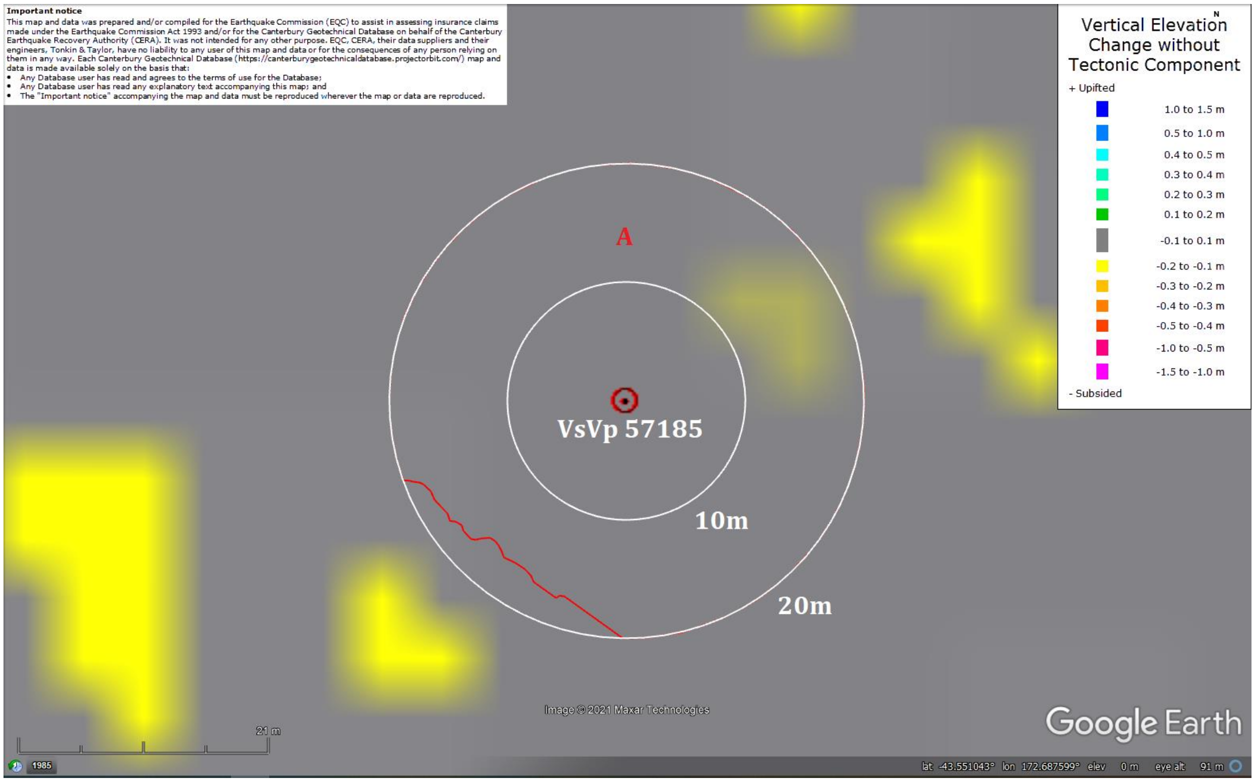

Figure 27: Ground surface subsidence without tectonic component for Dec 2011 Earthquake according to the LiDAR DEM.

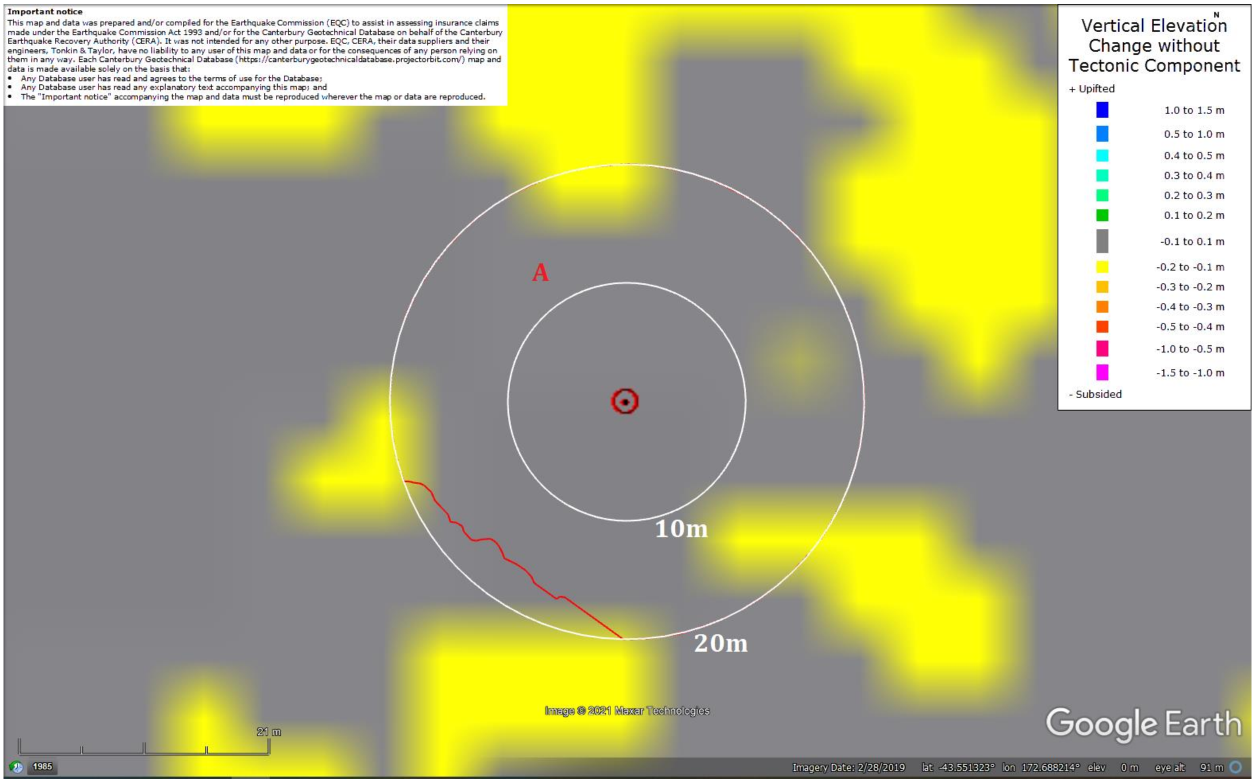

Figure 28: Ground surface subsidence without tectonic component for Canterbury Earthquake Sequence according to the LiDAR DEM.

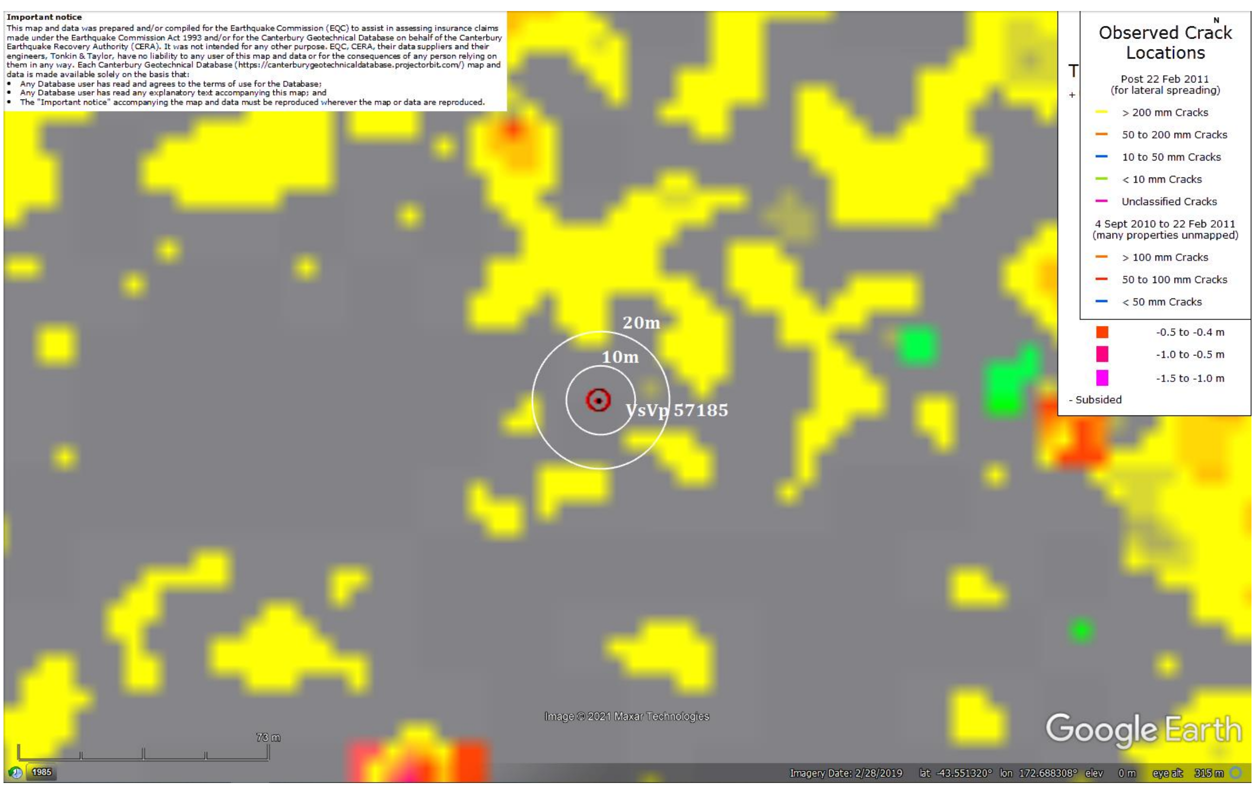

Figure 29: No lateral spreading for Canterbury Earthquake Sequence.

Figure 30: Vertical tectonic movements for Sep 2010 Earthquake.

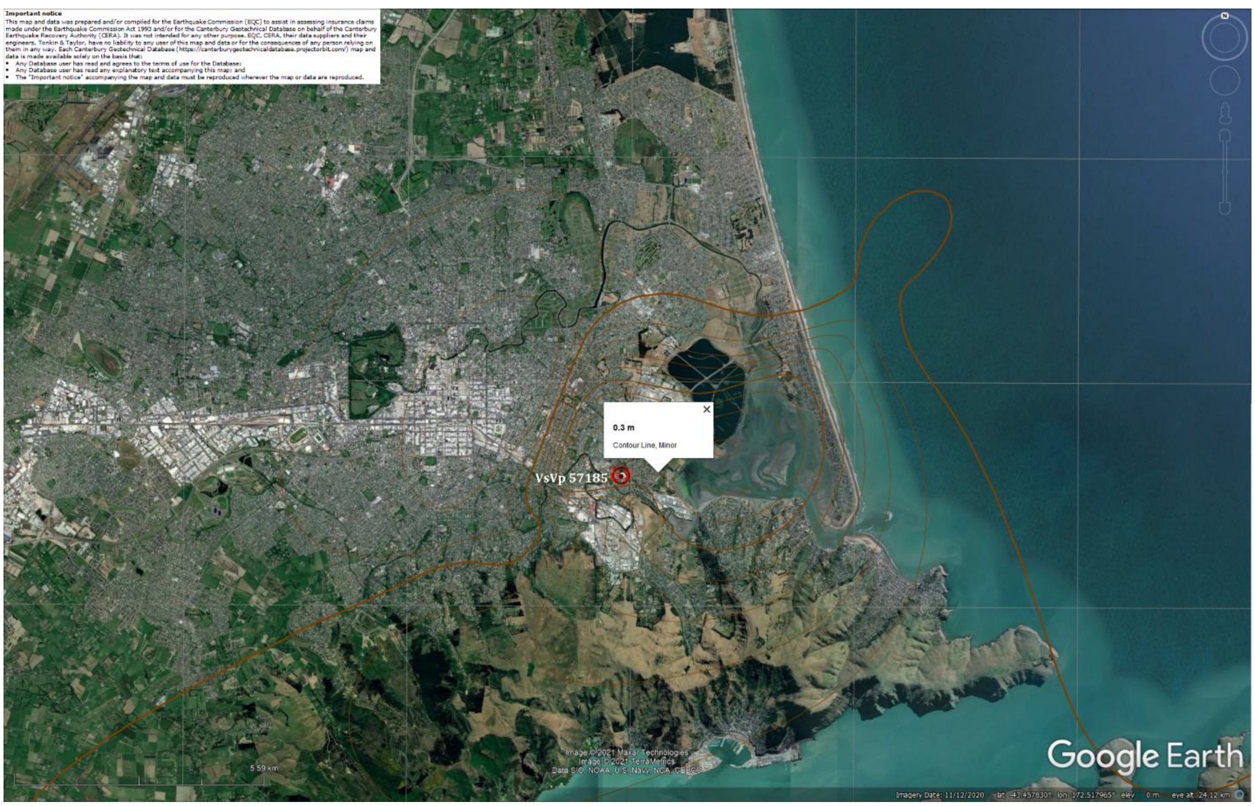

Figure 31: Vertical tectonic movements for Feb 2011 Earthquake.

Figure 32: Vertical tectonic movements for June 2011 Earthquake.

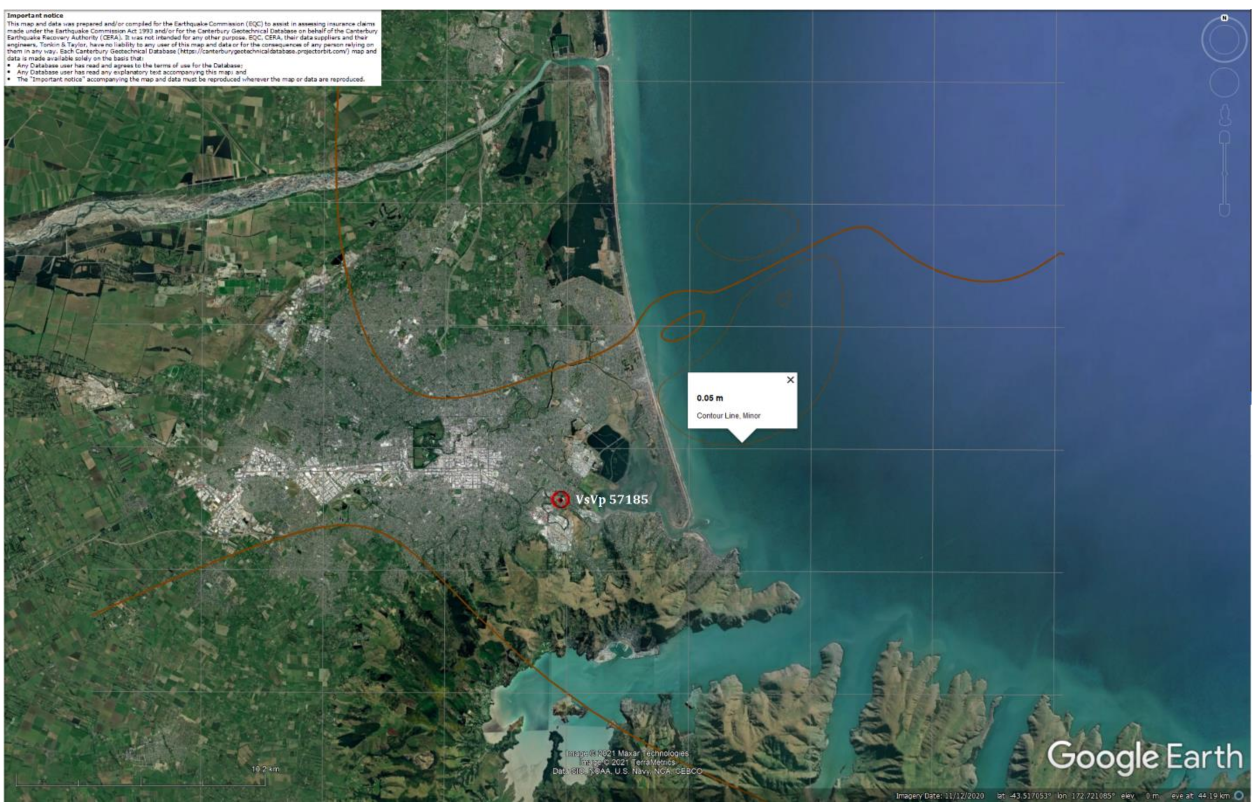

Figure 33: Vertical tectonic movements for Dec 2011 Earthquake.

Figure 34: Vertical tectonic movements for Canterbury Earthquake Sequence.

Figure 35: PGA for Sep-10 EQ (st. dev. = 0.350-0.375 ln units).

Figure 36: PGA for Feb-11 EQ (st. dev. = 0.375-0.400 ln units).

Figure 37: PGA for Jun-11 EQ (st. dev. = 0.400-0.425 ln units).

Figure 38: PGA for Dec-11 EQ (st. dev. = 0.425-0.450 ln units).

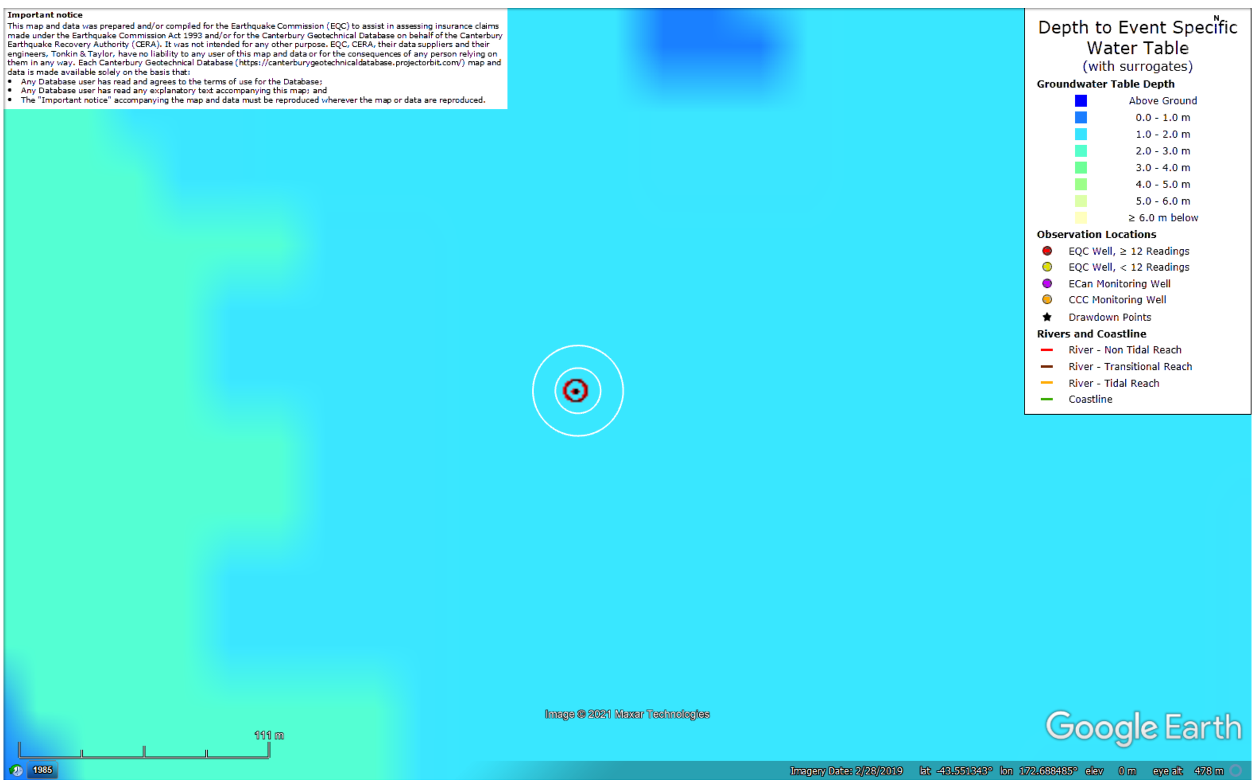

Figure 39: Depth to groundwater table for Sep-10 EQ.

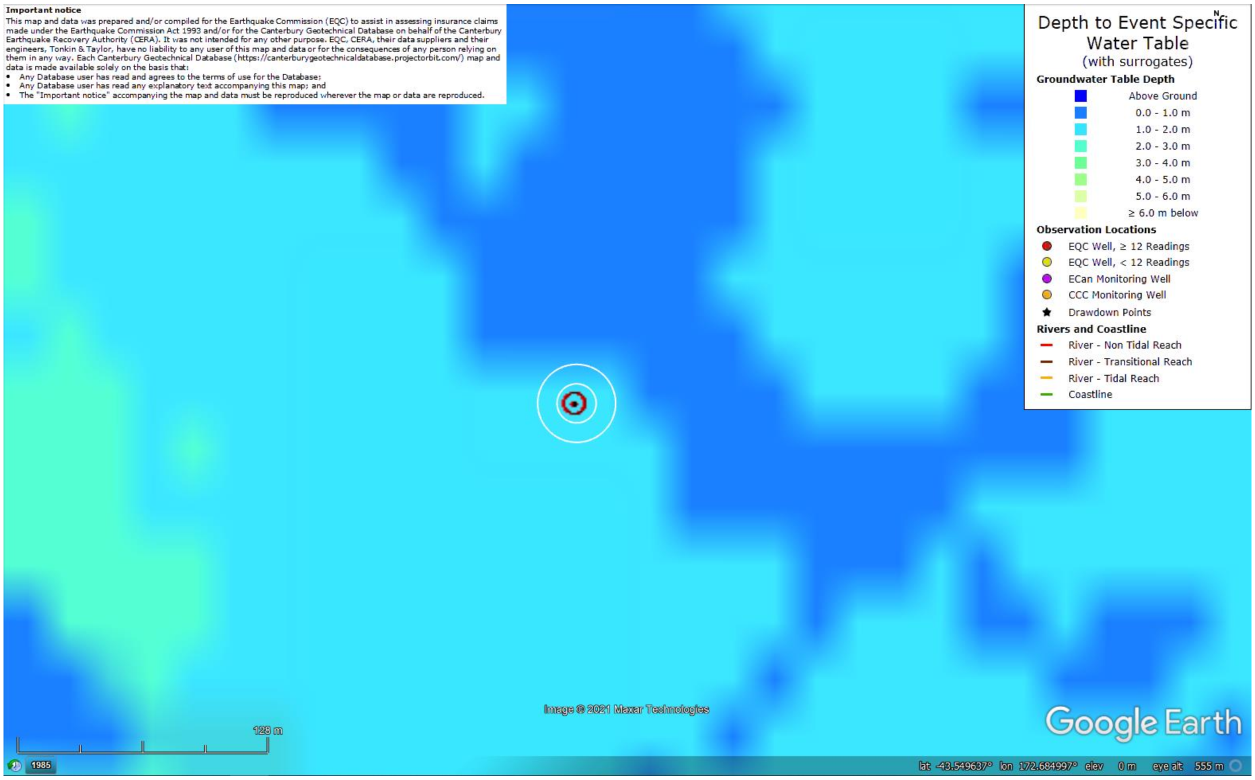

Figure 40: Depth to groundwater table for Feb-11 EQ.

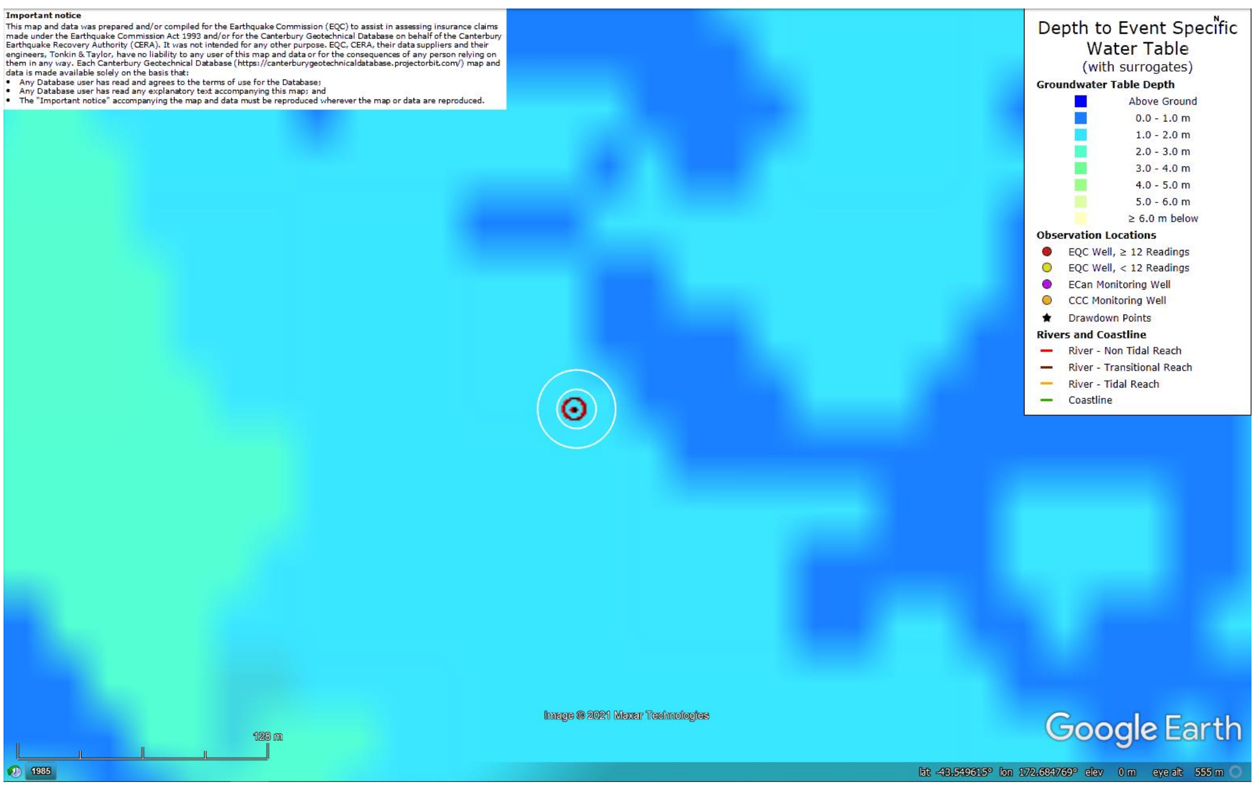

Figure 41: Depth to groundwater table for Jun-11 EQ.

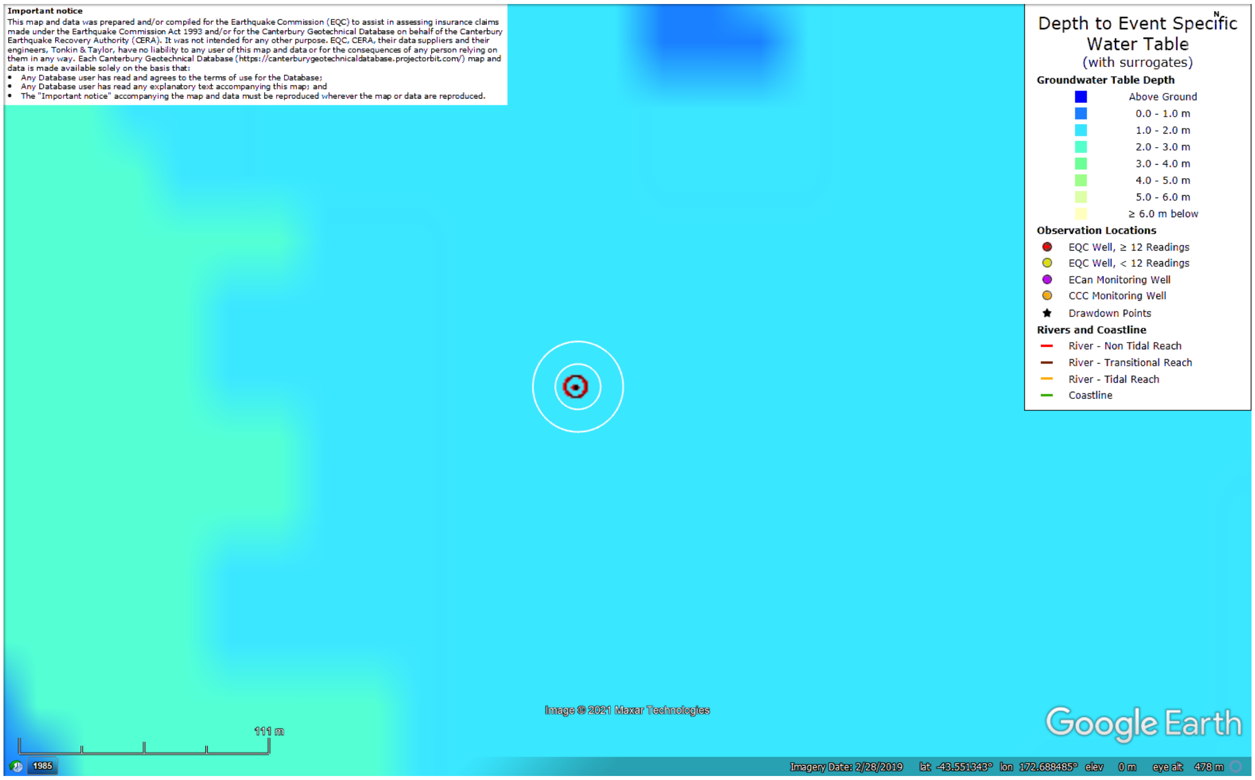

Figure 42: Depth to groundwater table for Dec-11 EQ.

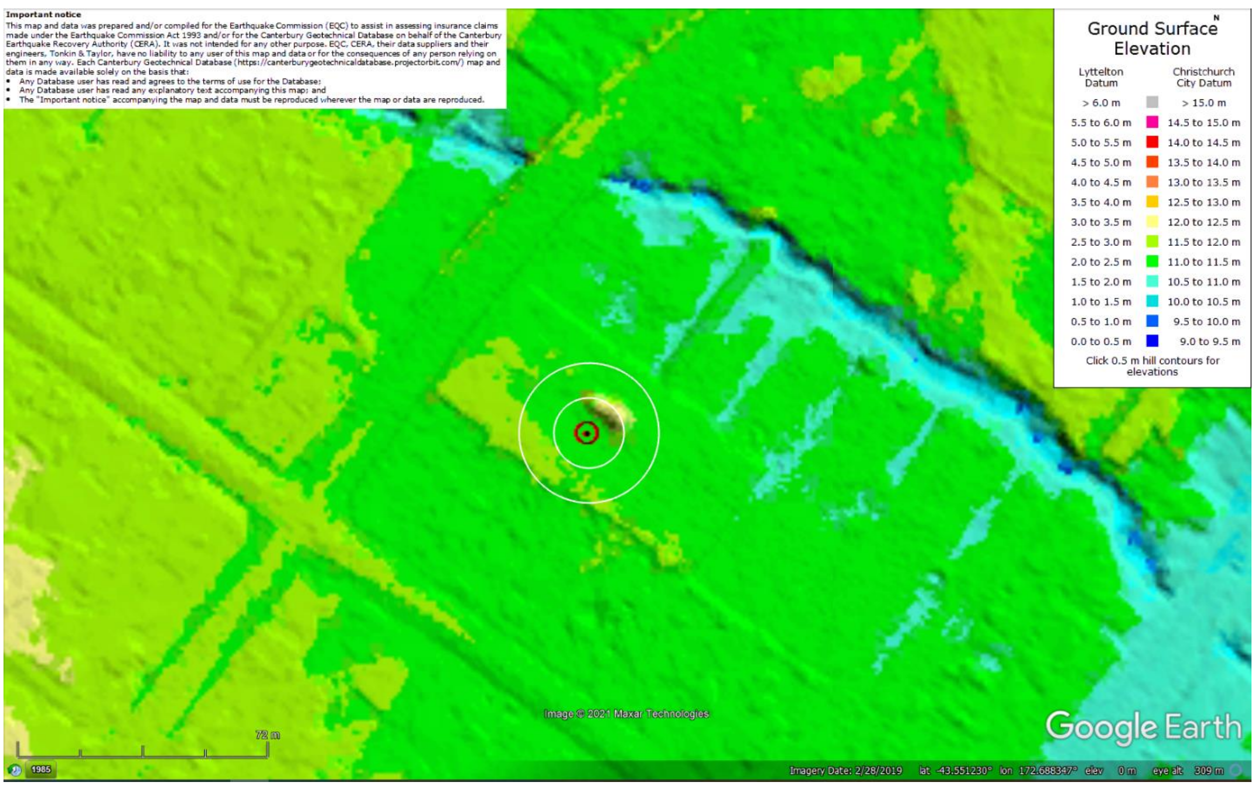

Figure 43: Ground surface elevation according to the Sep-11 LiDAR survey.

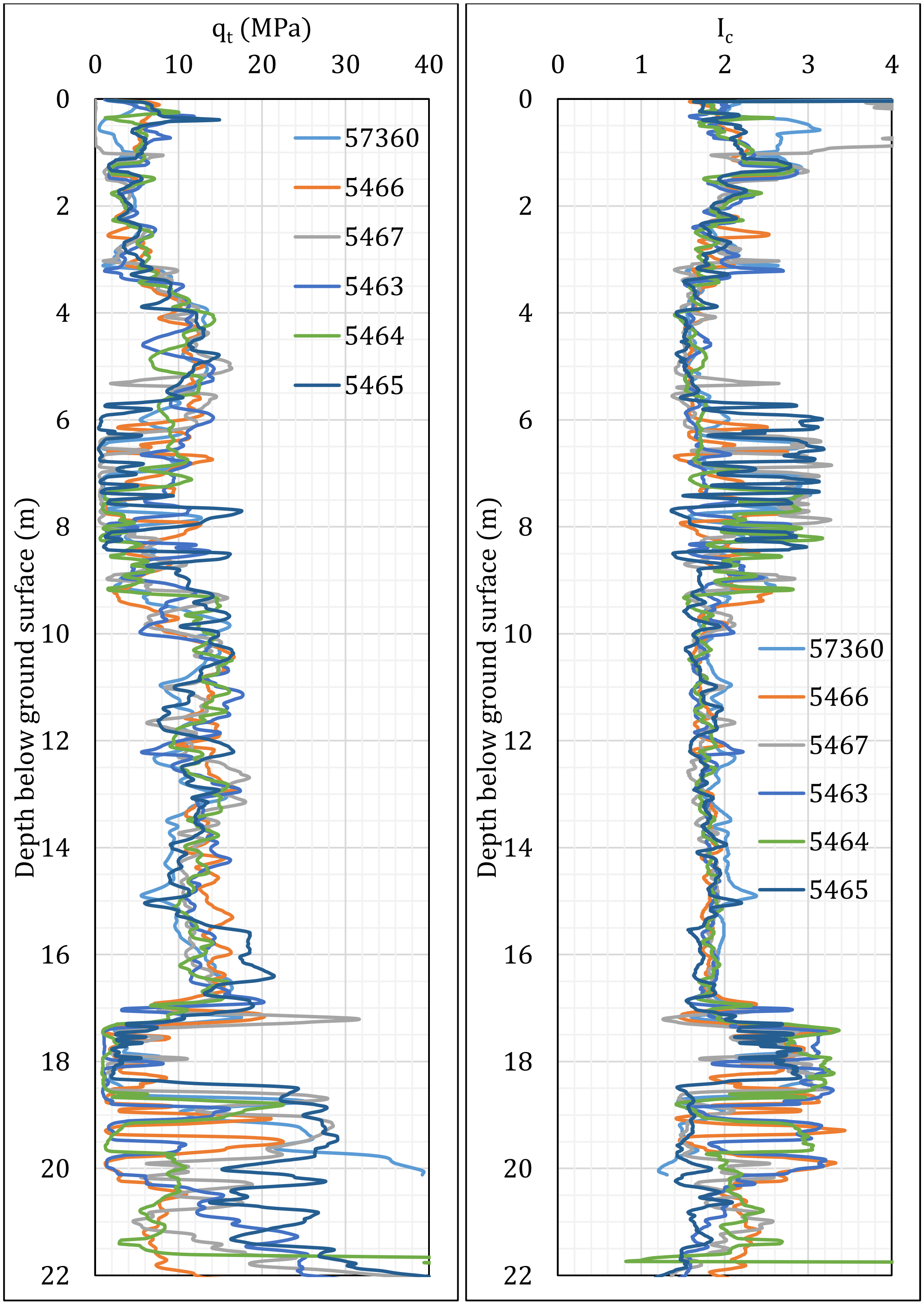

Figure 44: q_t and I_c profiles.

Note 5: The selection of CPTs for the area considered for settlement assessment (Figure 1) is based on the proximity of the CPTs to the considered areas. In accordance with that, the following table shows CPTs that were used for the volumetric settlement analysis in *Cliq v.3.0.3.2*, a CPT soil liquefaction software developed by GeoLogismiki. (The average volumetric settlements were reported in Table 8.)

Table 12: CPT profiles used in volumetric settlement analysis for Patch A selected for settlement assessment.

CPT ID No.	10-m buffer	20-m buffer
57360 (56738)	✓	✓
5466	✓	✓
5467	✓	✓
5463		
5464		✓
5465		✓

Table 13a: CPT-based results.

		CPT ID					
EQ Event	Parameter	57360	5466	5467	5463	5464	5465
Sep-10	S_{V1D} (mm)	82	91	84	91	100	99
	LSN	13	14	14	13	15	14
	LPI	4	4	4	3	4	4
	LPI_{ish}	1	0	1	0	0	1
	$D_{FS<1}$ (m)	2.74	2.46	2.05	2.89	4.76	2.74
Feb-11	S_{V1D} (mm)	233	266	231	266	279	240
	LSN	38	44	37	42	44	40
	LPI	31	36	30	36	37	33
	LPI_{ish}	23	27	24	27	28	26
	$D_{FS<1}$ (m)	1.42	1.43	1.52	1.49	1.48	1.50
Jun-11	S_{V1D} (mm)	153	170	156	179	190	179
	LSN	25	30	27	29	33	30
	LPI	13	15	13	15	17	16
	LPI_{ish}	8	10	9	10	12	11
	$D_{FS<1}$ (m)	1.98	1.69	1.74	1.74	1.66	1.64
Dec-11	S_{V1D} (mm)	64	75	63	69	78	77
	LSN	10	12	11	11	13	12
	LPI	3	3	3	2	4	3
	LPI_{ish}	1	1	1	1	1	1
	$D_{FS<1}$ (m)	2.76	8.28	2.06	2.91	4.79	2.75

Notes: $D_{FS<1}$ = Depth to the first liquefiable layer (FS_L<1) that is at least 200-mm thick, as determined by the Boulanger and Idriss (2016) liquefaction-triggering procedure (P_L=50%, C_{FC}=0.13, and $I_{c,cutoff}$ =2.6), and exported from *Cliq v.3.0.3.2*; undet. = the specified soil layer was not detected.

Note 6: Based on the borehole log (BH 57235, Figure 1), the groundwater table is at a depth of 1.2 m below the ground surface. The soil profile consists of (1) organic silty, OL, topsoil to a depth of 0.45 m, (2) silt, ML, the Yaldhurst member of the Springston formation, to a depth of 1.45 m, (3) organic silt, OL, the Yaldhurst member of the Springston formation to a depth of 1.65 m, (4) sandy silt, ML, the Yaldhurst member of the Springston formation, to a depth of 2.3 m, (5) fine sand, SP, the Yaldhurst member of the Springston formation, to a depth of 2.7 m, (6) silt, ML, the Yaldhurst member of the Springston formation, to a depth of 3.05 m, (7) fine sand, SP, of the Christchurch formation, to a depth of 6.95 m, (8) silt, ML, of the Christchurch formation, to a depth of 8.3 m, and (9) fine to medium sand, SP, of the Christchurch formation, to a depth of 15.65 m (the end of the borehole). According to BHs 6000 and 6001 (Figure 1), the SP layer extends to a depth of 16.5 m and is succeeded by (10) sandy silt, ML, of the Christchurch formation, to a depth of 17.9 m, (11) fine to medium sand, SP, of the Christchurch formation, to a depth of 19.5 m, and (12) silty fine sand, SM, of the Christchurch formation, to a depth of 20 m. The Yaldhurst members of the Springston formation contain trace organics.